Large Molecular Dynamics simulations of fullerene carbonization using composite symplectic integrators

G. J. Sibona [a] R. H. W. Hoppe [a,b] A. Revnic [a]

[a] *Institute of Mathematics, University of Augsburg, Germany.*

[b] *Department of Mathematics, University of Houston, U.S.A.*

Abstract

The modeling of the interaction between molecules and atoms by Molecular Dynamics (MD) has become an important tool during the last decade. Usually, the Störmer–Verlet scheme is used to integrate the equations of motion. In this paper, we study a higher order composite method (CM) at low extra computational cost performing simulations of the fullerene carbonization process. We found that the CM is suitable to analyze systems in which very accurate data are needed like the structural properties of the SiC layer growth.

Key words: Molecular dynamics, Tersoff potential, Verlet algorithm, composite symplectic integrators.

1 Introduction

We consider the coating of surfaces by thin films, a technological process to produce innovative materials with tailored structural properties. Their importance lays in its multiple applications, in particular in the microelectronics industry for the production of more efficient components. In this context, silicon carbide (SiC) has attracted a lot of attention during the past decade. Crystalline SiC layers on silicon (Si) are usually grown by chemical vapor deposition (CVD) techniques, but it was reported that the fullerene carbonization of Si is essential for growing high-quality, uniform, low-temperature cubic SiC thin films without introducing unwanted species [1]. Although the thermal reaction of C_{60} molecules with Si surfaces was studied using various techniques, little is known about the mechanism leading to the breaking of the molecule and the formation of the silicon carbide. In this framework, we have performed

Molecular Dynamics (MD) simulations to analyze the structural properties of the SiC layer during the growth process [2].

The MD method is one of the computer simulation methods employed to study the properties of a many-particle system. Since it usually involves the computation of the interatomic potentials between many particles, it is necessary to establish new efficient techniques. Using a suitable potential with multibody functions, empirical MD simulations can considerably shorten the computational time while yielding physical properties with desirable accuracy. In this context, the Tersoff potential [15] has been applied with great success. Another way to reduce the computational time of the simulations is to improve the numerical integration of the equations of motion. In general, the Störmer-Verlet scheme is used representing a symplectic method of second order. The aim of this work is to introduce a new method for the numerical integration of the equations of motion by increasing the order at low extra computational cost.

The paper is organized as follows: In section 2, we briefly address the process of fullerene carbonization by the bombardment of silicon substrates with C_{60} molecules. This is followed by a description of the molecular dynamics approach using the Tersoff potential, given in section 3. For the integration of the equations of motions, in section 4 we briefly recall the usual Störmer-Verlet scheme and introduce the higher order composition method. Section 5 is devoted to describe the parallel scheme used in the implementation of the Molecular Dynamics code. Finally, in section 6 we present the results of MD simulations of the fullerene carbonization and discuss the pros and cons of the composite method.

2 The process of fullerene carbonization

The synthesis of high-quality SiC by fullerene carbonization can be done in an ultra high vacuum chamber which allows the controlled simultaneous deposition of fullerenes and silicon. Figure 1 gives a schematic representation of that vacuum chamber.

Using an effusion cell, C_{60} fullerene molecules are deposited on a silicon substrate that is kept at a fixed temperature. After the impact on the hot surface of the substrate, the fullerenes fragmentate and the carbon atoms interact with the silicon atoms.
If only fullerenes are deposited, due to diffusion processes cavities form at the lower interface of the growing SiC layer. Therefore, in addition to the C_{60} molecules, gaseous silicon is deposited simultaneously which is taken care of by an electron beam evaporator. For the in-situ analysis and the control of

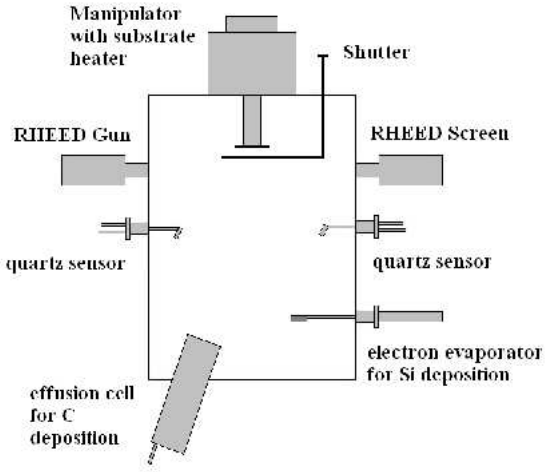

Fig. 1. Ultra high vacuum chamber for SiC synthesis by fullerene carbonization.

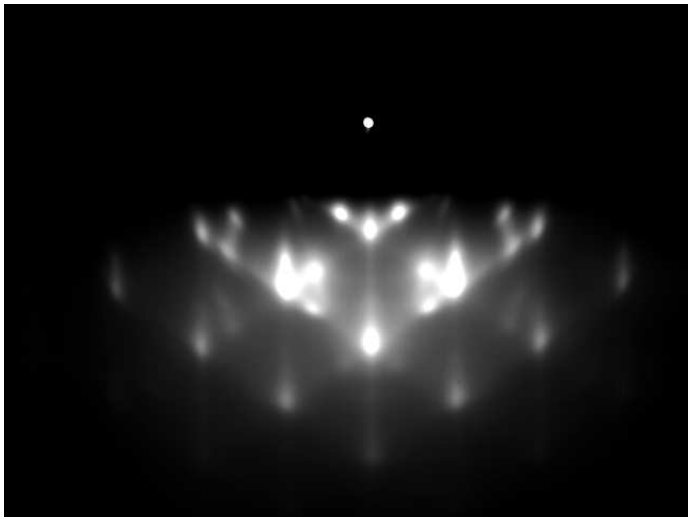

Fig. 2. RHEED-diffraction pattern of a 3C-SiC layer along the [110] direction.

the SiC growth, the vacuum chamber is equipped with a RHEED-analytics (Reflection High Energy Electron Diffraction). This allows to study the influence of the process parameters on the growth process during deposition. Figure 2 shows the RHEED-diffraction pattern of a 3C-SiC layer along the [110] direction.

3 Modeling and simulation by molecular dynamics

In molecular dynamics, the behavior of a system of N particles is modeled by Newton's equations of motion

$$m_i \frac{d\,\mathbf{v}_i}{d\,t} = -\nabla_i V(\mathbf{r}_1, ..., \mathbf{r}_N) \ , \qquad (1)$$
$$\frac{d\,\mathbf{r}_i}{d\,t} = \mathbf{v}_i \ , \ 1 \le i \le N \ ,$$

where $\mathbf{r}_i, \mathbf{v}_i$, and m_i stand for the position vector, the velocity vector, and the mass of the i-th particle, and $V(\mathbf{r}_1, ..., \mathbf{r}_N)$ refers to the potential energy of the system as a function of the position vectors of all particles. The negative gradient $-\nabla V_i = -(\frac{\partial V_i}{\partial x_i}, \frac{\partial V_i}{\partial y_i}, \frac{\partial V_i}{\partial z_i})^T$ corresponds to the force $\mathbf{F}_i$ acting on the i-th particle.
We note that (1) represents a Hamiltonian system with respect to the Hamiltonian

$$H(\mathbf{r}_1, ..., \mathbf{r}_N, \mathbf{v}_1, ..., \mathbf{v}_N) \ = \ \frac{1}{2} \sum_{i=1}^{N} m_i \ \mathbf{v}_i^2 \ + \ V(\mathbf{r}_1, ..., \mathbf{r}_N) \qquad (2)$$

which describes the total energy of the system.
The physics of the system is completely determined by the function V which comprises all exterior and interatomar potentials.
For the fullerene carbonization over a Si surface, suitable choices are Brenner- and Tersoff-type potentials (cf., e.g., [12,15–17]), which are similar to the Morse-like potential, but explicitly involve the bond-order of atoms. The approach assumes that the energy V_i of an atom i in a configuration of N atoms is given by

$$V \ = \ \frac{1}{2} \sum_{i \neq j} V_{ij} \ = \ \frac{1}{2} \sum_{i \neq j} f_C(r_{ij}) \ [\ f_R(r_{ij}) \ + \ b_{ij} f_A(r_{ij}) \ ] \ . \qquad (3)$$

Here, $r_{ij} := \mid \mathbf{r}_i - \mathbf{r}_j \mid \ , \ 1 \le i \neq j \le N$, and $f_C(\cdot)$ is the cut-off function

$$f_C(r) \ := \ \begin{cases} 1 \quad , & r < R - D \\ \frac{1}{2} \ - \ \frac{1}{2} \sin\left(\frac{\pi}{2} \frac{r-R}{D}\right) \quad , & R - D \le r \le R + D \\ 0 \quad , & R + D < r \end{cases} \ , \qquad (4)$$

whereas $f_A(\cdot), f_R(\cdot)$ denote attractive and repulsive potentials, respectively,

$$f_A(R) \ := \ - \ A \exp\left(- \ \lambda_1 \ r\right) \quad , \quad f_R(R) \ := \ B \exp\left(- \ \lambda_2 \ r\right) \ . \qquad (5)$$

Moreover, the bond-order parameter b_{ij} is chosen as a monotonically decreasing function of the number of neighbors of the atoms i and j according to the bond-order-concept which states that the more neighbors an atom has, the

weaker the bond to each neighbor:

$$b_{ij} \;:=\; (\; 1 \;+\; \beta^m \; \xi_{ij}^m \;)^{-\frac{1}{2m}} \;. \tag{6}$$

Here, ξ_{ij} is the effective coordination number given by

$$\begin{aligned} \xi_{ij} &:= \sum_{k \neq i,j} f_C(r_{ik}) \; g(\theta_{ijk}) \; \exp\; (\lambda_3^3 \; (r_{ij} - r_{ik})^3) \;, \\ g(\theta) &:= 1 \;+\; \frac{c^2}{d^2} \;-\; \frac{c^2}{d^2 + (h - \cos\,\theta)^2} \;, \end{aligned} \tag{7}$$

where θ_{ijk} represents the bond angle formed by the bond between atom i and atom j and the bond between atom j and atom k.
Note that the weighting factor $\exp\,(\lambda_3^3(r_{ij} - r_{ik})^3)$ takes into account the relative distance between different neighbors: a weaker bond (longer distance r_{ik}) will be considerably more weakened by a stronger bond (shorter distance r_{ij}) than vice versa. Furthermore, the function g, depending on the bond angle, is another weighting factor which is chosen such that it stabilizes the crystallographic structure with regard to shear forces.
Note that the weighting factors do not occur in the classical Tersoff potentials but have been introduced to improve the quality of the model for the specific system under consideration.
The parameters A, B, c, d, h, m, β, and $\lambda_i, 1 \leq i \leq 3$, in (5),(6),(7) are fitted both by using experimentally obtained data such as elasticity modules and lattice specific constants as well as with regard to structural energies (e.g., surface and defect energies) and interatomar forces computed by means of ab-initio quantum mechanical calculations.
Ab-initio methods consider every atom as a many particle system consisting of the atomic nucleus and the surrounding electrons. The many particle system is then solved by self consistent pseudopotential calculations based on the density functional theory (cf., e.g., [11]). However, such computations require an enormous amount of work and therefore, they have been carried out for less particles than are used in the molecular dynamics approach.

We have selected a larger cutoff parameter (R) for the carbon atoms in order to extend the range of the interaction. This is because the interaction between the second-neighbor surface atoms must account for some surface structural features [4]. The value was selected to describe properly the melting point of the fullerene.

Parameters	C	Si
A (eV)	1393.6	1830.8
B (eV)	346.7	471.18
λ (Å^{-1})	3.4879	2.4799
μ (Å^{-1})	2.2119	1.7322
β	1.5724e-7	1.0999e-6
n	0.72751	0.78734
c	38049	100390
d	4.384	16.218
h	-0.57058	-0.59826
R (Å)	2.35	2.85
D (Å)	0.15	0.15

Table 1
Parameters for carbon and silicon used in the Tersoff potential.

4 Symplectic Methods

For the numerical integration of the Hamiltonian system (1), symplectic integrators are well suited due to conservation of energy [14]. In fact, a backward analysis [7,13] shows that the total energy is well preserved for exponentially long time horizons $T = \Delta t \exp(C/2\Delta t)$:

$$\begin{aligned} &H(\mathbf{r}_1(k\Delta t), ..., \mathbf{r}_N(k\Delta t), \mathbf{v}_1(k\Delta t), ..., \mathbf{v}_N(k\Delta t)) \;= \\ &= H(\mathbf{r}_1(0), ..., \mathbf{r}_N(0), \mathbf{v}_1(0), ..., \mathbf{v}_N(0)) \;+\; O((\Delta t)^p) \quad , \quad k\Delta t < T \;, \end{aligned}$$

where Δt is the time step-size and p refers to the order of consistency of the integrator.
The most commonly used method in molecular dynamics is the Störmer–Verlet scheme, a standard symplectic integrator of order $p = 2$:

$$\mathbf{r}_i(t + \Delta t) - 2\mathbf{r}_i(t) + \mathbf{r}_i(t - \Delta t) = \Delta t^2 \frac{1}{m_i} \mathbf{F}_i(t) \tag{8}$$

which is in fact the most natural discretization of Newton's equations $m_i \ddot{\mathbf{r}}_i = \mathbf{F}_i$.

The two-term recursion (4.1) can be easily modified giving the classical formulation of the Störmer–Verlet scheme in molecular dynamics.

$$\mathbf{r}_i(t+\Delta t) = \mathbf{r}_i(t) \; + \; \Delta t \; \mathbf{v}_i(t) \; + \; \frac{1}{2} \; \frac{(\Delta t)^2}{m_i} \; \mathbf{F}_i(t) \; , \tag{9}$$

$$\mathbf{v}_i(t+\Delta t) = \mathbf{v}_i(t) \; + \; \frac{1}{2} \; \frac{\Delta t}{m_i} \; (\; \mathbf{F}_i(t) \; + \; \mathbf{F}_i(t+\Delta t)) \quad , \quad 1 \leq i \leq N \; .$$

A time-step of the Störmer–Verlet algorithm is shown in Figure 3.

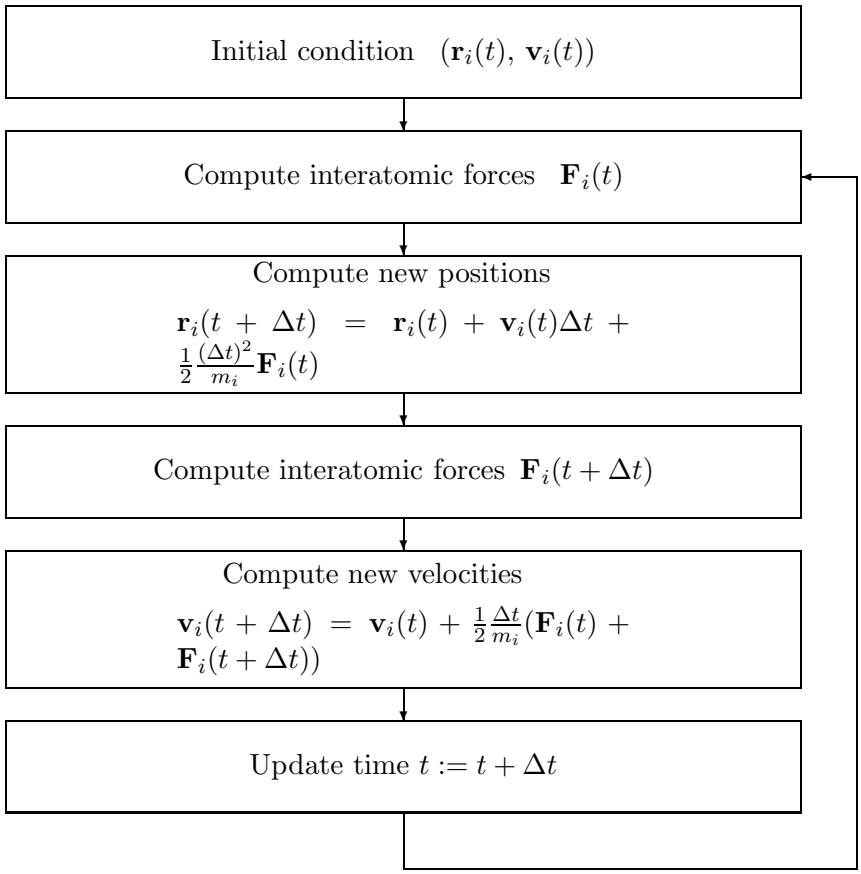

Fig. 3. Time-step of the Störmer–Verlet algorithm.

Lemma 1 *The Störmer-Verlet scheme can be written as an explicit one-step method*

$$\Phi_{\Delta t}^{SV} \; : \; (\mathbf{r}_i(t), \mathbf{v}_i(t)) \; \longmapsto \; (\mathbf{r}_i(t+\Delta t), \mathbf{v}_i(t+\Delta t)) \quad . \tag{10}$$

PROOF. Introducing the velocity approximation $\mathbf{v}_i(t + \frac{\Delta t}{2})$ at the midpoint of the time interval, we get

$$\mathbf{v}_i(t + \frac{\Delta t}{2}) = \mathbf{v}_i(t) \; + \; \frac{\Delta t}{2} \; \frac{1}{m_i} \; \mathbf{F}_i(t) \quad , \tag{11}$$

$$\mathbf{r}_i(t+\Delta t) = \mathbf{r}_i(t) \ + \ \Delta t \ \mathbf{v}_i(t+\frac{\Delta t}{2}) \quad ,$$
$$\mathbf{v}_i(t+\Delta t) = \mathbf{v}_i(t+\frac{\Delta t}{2}) \ + \ \frac{\Delta t}{2} \ \frac{1}{m_i} \ \mathbf{F}_i(t+\Delta t) \quad . \qquad \Box$$

It is interesting to notice that for the implementation of the Störmer–Verlet method, the one–step formulation (4.4) is numerically more stable than the two–term recursion (4.1).

A particular procedure for constructing an integration method of higher order is by composition of a lower order one. The aim is to increase the order of a lower order method, while preserving its properties such as symplecticity, symmetry, and straightforward implementation. In the following, we will use the ideas presented in [8] and [9] in order to obtain a method of order 4 based on the composition of three Störmer–Verlet methods.

Theorem 2 *Consider the composition method*

$$\Phi^{CM}_{(\alpha_1+\alpha_2+\alpha_3)\Delta t} \ := \ \Phi^{SV}_{\alpha_1\Delta t} \odot \Phi^{SV}_{\alpha_2\Delta t} \odot \Phi^{SV}_{\alpha_3\Delta t} \quad . \tag{12}$$

Then there holds:

(i) If $\alpha_i \in \mathbb{R}$, $1 \leq i \leq 3$, *are chosen according to*

$$\begin{aligned} &\alpha_1 \ + \ \alpha_2 \ + \ \alpha_3 = 1 \quad , \\ &\alpha_1^3 \ + \ \alpha_2^3 \ + \ \alpha_3^3 = 0 \quad , \end{aligned} \tag{13}$$

the composition method $\Phi^{CM}_{\Delta t}$ *has at least the order 3.*

(ii) If in addition to (13) there holds

$$\alpha_1 = \alpha_3 \quad , \tag{14}$$

the composition method $\Phi^{CM}_{\Delta t}$ *has at least the order 4.*

PROOF. The Störmer-Verlet method is of order 2, i.e., denoting by $\Phi^{exact}_{\Delta t}(\mathbf{w})$ the exact solution, for sufficiently smooth $\mathbf{w}$ we have

$$\Phi^{SV}_{\Delta t}(\mathbf{w}) \ = \ \Phi^{exact}_{\Delta t}(\mathbf{w}) \ + \ C(\mathbf{w}) \ (\Delta t)^3 \ + \ O((\Delta t)^4) \quad .$$

Consequently, in view of (12)

$$\Phi^{CM}_{(\alpha_1+\alpha_2+\alpha_3)\Delta t}(\mathbf{w}) = \Phi^{exact}_{(\alpha_1+\alpha_2+\alpha_3)\Delta t}(\mathbf{w}) \; + \\ (\alpha_1^3+\alpha_2^3+\alpha_3^3)\; C(\mathbf{w})\; (\Delta t)^3 \; + \; O((\Delta t)^4) \quad ,$$

which shows that assertion (i) holds true.
Moreover, the Störmer-Verlet scheme is symmetric, i.e.,

$$\Phi^{SV}_{\Delta t} \; = \; (\Phi^{SV}_{-\Delta t})^{-1} \quad .$$

It follows readily from (12) that the composition method is as well symmetric if (14) is satisfied. Since the order of a symmetric method is always an even number (see, e.g., [10]), this proves (ii). □

Solving the system (4.6)–(4.7), we obtain

$$\begin{aligned} \alpha_1 &= 1.3512072 \\ \alpha_2 &= -1.7024145 \\ \alpha_3 &= 1.3512072. \end{aligned} \tag{15}$$

The implementation of this method is straightforward. Once a Störmer–Verlet (SV) routine is introduced, the CM consists of calling this routine three times with different time steps, using the scaling parameters given by (15).

This means, the method takes two positive intermediate steps $1.3512072 \times \Delta t$ and one negative intermediate step $-1.17024145 \times \Delta t$, as shown in Figure 4.

5 Parallel Implementation

The most time-consuming step in the molecular dynamics simulations is the computation of the interacting forces. Since the interactions for distances $r_{ij} > R$ are neglected, we implemented a "particle-in-cell" method. Based on this we can assign a certain number of cells to a processor in a multi-processor machine so that the computation of the interacting forces and the movement of the particles can take place in parallel. In particular the computing area is divided in cells in such a manner that for each particle i all neighbors j located at distances $r_{ij} < R$ are either in the same cell or in one of the first neighboring cells. If all particles in the adjoining cells are considered, then the interacting forces for such particles are computed. For this reason, additional neighbor lists are created to consider only the next neighbors. To reduce the

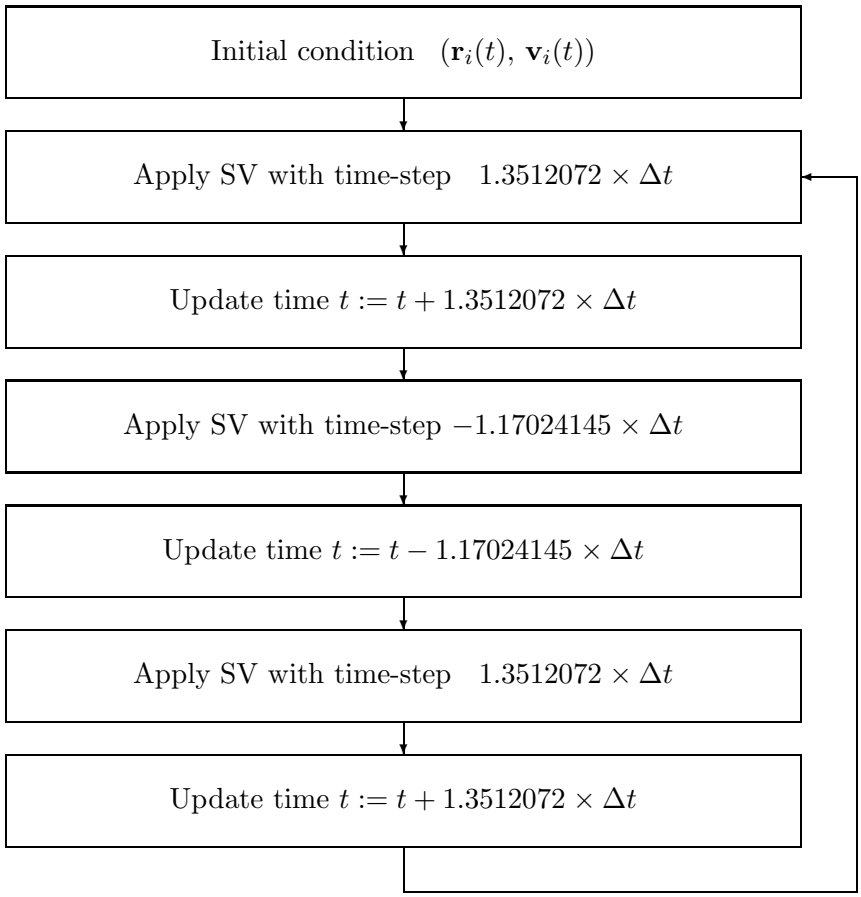

Fig. 4. Implementation of the composite method.

cost of the computation of the neighbor lists, we can use them for several successive time steps considering not only the neighbors j with $r_{ij} < R$, but extending the list by a safety margin δ_S. If. for example, the maximum speed of the particles is v_{max}, then the neighbor lists must be computed again after $\delta_S/(2v_{max}\Delta t)$ time steps.

The parallel version of the algorithms have been implemented on the Itanium cluster of the University of Houston Computing Center using the MPI (Message Passing Interface) library. To judge the performance of the parallel approach, we have computed the speed-up factor and the efficiency of the simulations [18]. Given a p-processor simulation of total time $T(p)$, the speed-up factor S can be defined as:

$$S = \frac{T(1)}{T(p)} \tag{16}$$

and the efficiency

$$E = \frac{S}{p}. \tag{17}$$

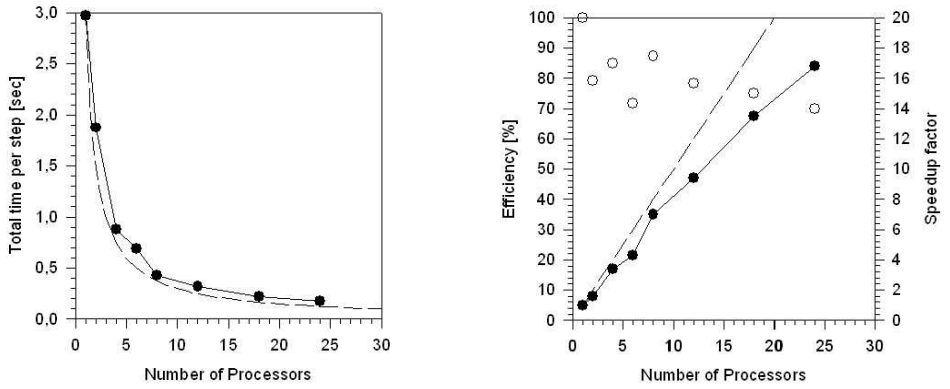

Fig. 5. Parallel performance (left), speed-up and parallel efficiency (right) as a function of the number of processors

Figure 5 shows the reduction of the total time per step while increasing p (left) as well as the parallel acceleration (speed-up) and the parallel efficiency (right) of the parallelized algorithms when using up to 24 programmable processors. In the figure, the dashed lines correspond to the perfect theoretical conditions where there is no extra time due to communications between the processors.

6 Simulation results

The investigation of the structural properties of the SiC layer during its growth requires to study the dispersion of the carbon atoms after the fragmentation of the C_{60} molecule. A parameter that gives information about the behavior of the carbon atoms is the mean radius of the fullerene molecule. It has to increase while the carbon atoms start to interact with the silicon atoms rearranging with them in the SiC configuration.
As a first approach, we want to test the accuracy of the numerical methods performing simulations of the evolution of a single fullerene molecule at 300K. We use the MD++ library developed at the University of Augsburg to analyze the deposition of thin films [3]. The code makes use of the well known cell-partition method together with the nearest neighbor concept.
The results are displayed in Figure 6 for different time steps. The mean radius oscillates around its stable value due to the random initial velocities of the carbon atoms. As we decrease the time step, the curves tend to its asymptotic value considered for the rest of this paper as the exact result. As can be expected, the Störmer-Verlet scheme introduces less error for bigger time steps, but what happens for lower time steps? This can be seen in Figure 7 where the difference to the exact value is shown at time $t = 10$fs. Here, the CM error

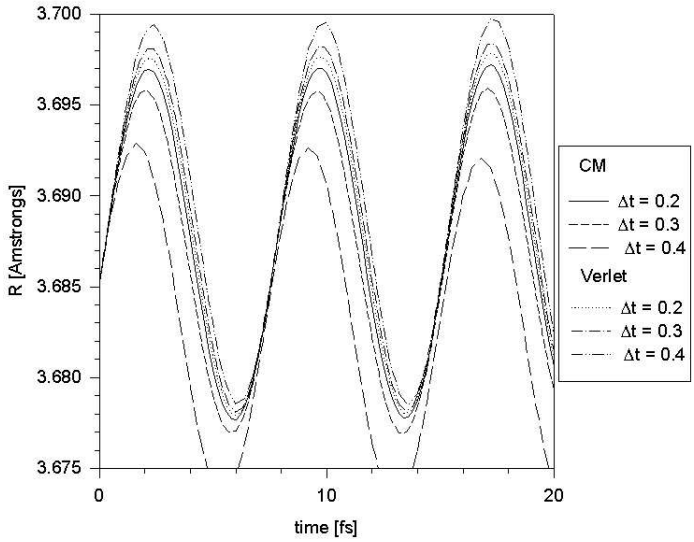

Fig. 6. Mean radius of the fullerene at 300K computed for different time steps.

decreases faster than the Störmer-Verlet error. In particular, we found that in this simulation it is worth to use the composite method for time steps lower than 0.1fs.

For the analysis of the long time behavior of the molecules using larger time steps, the Verlet scheme performs better, as for example in the surface diffusion of atoms, the bulk diffusion of defects or the growth of thin layers by the bombardment of high energy particles, where the mean behavior of the atoms is needed. But there are other cases where one is interested in very accurate values like the bond angles, binding energies, or the molecular structure and topology. This can be seen properly, if we simulate the behavior of the fullerene molecule at high temperatures. Figure 8 shows the evolution of the mean radius of the fullerene for different time steps using both integration methods. The atoms of the molecule start to dissociate after a couple of oscillations around its mean value. Here, the evolution differs completely for higher time steps, and even for $\Delta t = 10^{-5}$ the exact curve is not reached.

As far as the simulation of the fullerene carbonization is concerned, Figure 9 displays a fullerene molecule impinging on a silicon substrate. The interaction between the fullerene molecule and the silicon substrate is modelled by an arrangement of 7x7x10 Si atoms representing an area of $1.4510^{-15}cm^2$. Figure 10 displays the behavior of the mean radius of the fullerene during the impinging process. The fullerene is initially at a temperature of 400K and the silicon substrate at 1100K resembling the values used in experiments [5,6]. The curves show how the radius behaves after the impact of the fullerene, before the carbon atoms start to disperse over the substrate. Again, the curves differ

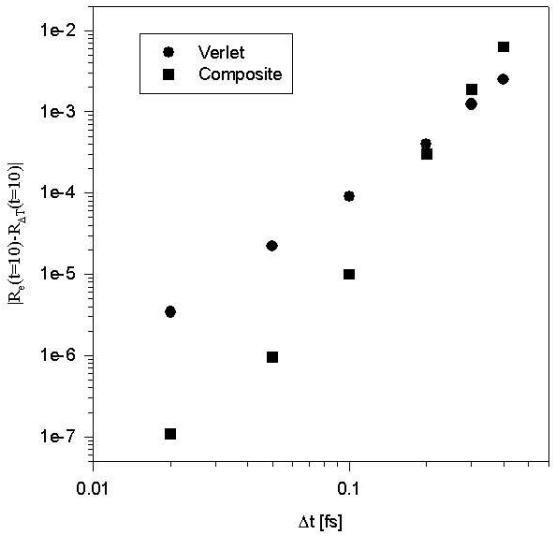

Fig. 7. Difference with respect to the exact mean radius at time $t = 10$fs for the fullerene at 300K as a function of the time step

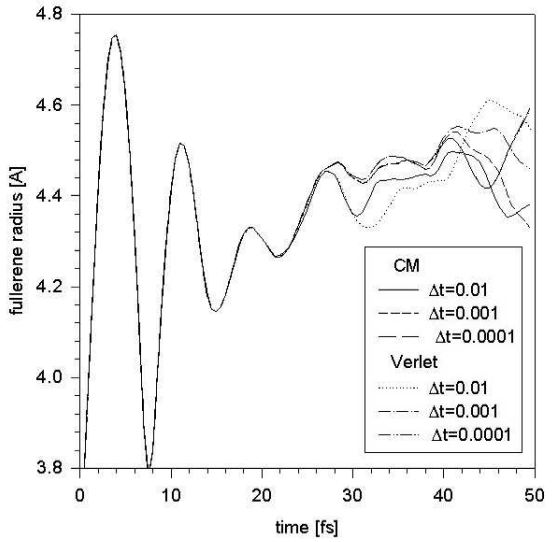

Fig. 8. Mean radius of the fullerene at 1100K computed with different time steps.

for different time steps underlining that a finer discretization must be used to find the exact behavior.

Fig. 9. Impinging of the fullerene molecule on a silicon substrate.

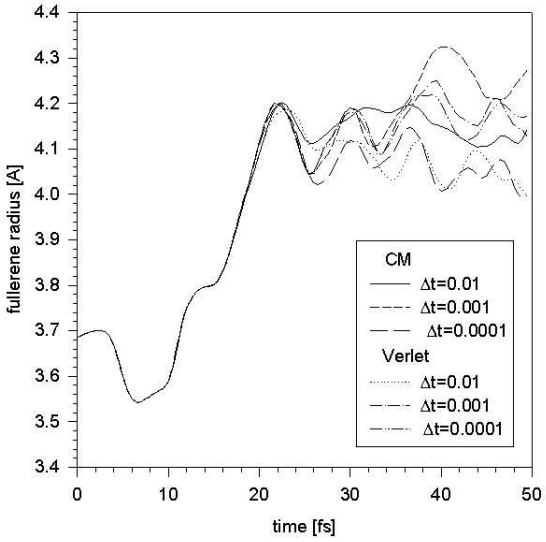

Fig. 10. Mean radius of the fullerene at 400K impacting with a kinetic energy of 500eV at a silicon substrate originally at 1100K.

7 Conclusions

We have derived a composite symplectic integrator for the numerical solution of Newton's equations of motions of many particle systems as they typically arise in Molecular Dynamics. The composite scheme is based on three steps with the well established Störmer-Verlet method and asymptotically achieves the convergence order 4 instead of 2 as for the underlying Störmer-Verlet method.
The computational results carried out for the process of SiC synthesis by fullerene carbonization clearly show the usefulness of the composite method for simulations with small time steps where fine details have to be detected. On the other hand, for long time simulations with larger time steps, where the asymptotics of the composite method is not reached, the Störmer-Verlet method is more appropriate.

Acknowledgements

This work has been supported by the German National Science Foundation (DFG) within the DFG-funded Collaborative Research Field SFB 438.

References

[1] M. De Seta, N. Tomozeiv, D. Sanvitto, and F. Evangelisti. SiC formation on Si(100) via C_{60} precursor. *Surf. Sci.* **460**, 2000) 203–213.

[2] G.J. Sibona, S. Schreiber, R.H.W. Hoppe, B. Stritzker, and Adrian Revnic; Numerical Simulation of the Production Processes of Layered Materials. *Materials Science in Semiconductor Processing* **6** (2003) 71–76.

[3] R.H.W. Hoppe, G. Sibona, A. Revnic, and D. Schweitzer; Numerical simulation of ion beam assisted deposition of thin cubic boron nitride films. submitted to *Computational Material Science* (2005).

[4] X. Luo, G. Qian, W. Fei, E.G. Wang, and C. Chen; Systematic study of β-SiC surface structures by molecular-dynamics simulations. *Phys. Rev. B* **57** (1998) 9234–9240.

[5] K. Volz, S. Schreiber, M. Zeitler, B. Rauschenbach, B. Stritzker, and W. Ensinger. Structural investigations of silicon carbide films formed by fullerene carbonization of silicon. *Surf. Coat. Tech.* **122** (1999) 101–107.

[6] K. Volz, S. Schreiber, J.W. Gerlach, W. Reiber, B. Rauschenbach, B. Stritzker, W. Assmann, and W. Ensinger. Heteroepitaxial growth of 3C-SiC on (100) silicon by C_{60} and Si molecular beam epitaxy. *Mat. Sci. & Eng. A* **289** (2000) 255–264.

[7] E. Hairer. Backward analysis of numerical integrators and symplectic methods. *Annals of Numerical Mathematics* **1** (1994) 107.

[8] H. Yoshida. Construction of higher order symplectic integrators. *Phys. Lett. A* **150** (1990) 262–268.

[9] R.I. McLachlan and G.R.W. Quispel. Splitting methods. *Acta Numerica* **11** (2002) 341–435.

[10] E. Hairer, Ch. Lubich, and G. Wanner. Geometric Numerical Integration. In: *Structure–Preserving Algorithms for ODEs*, Springer Verlag, 2002.

[11] M. Bockstedte, A. Kley, J. Neugebauer, M., and Scheffler. Density-functional theory calculations for polyatomic systems: electronic structure, static and elastic properties and ab initio molecular dynamics. *Comp. Phys. Commun.* **107** (1997) 187–222.

[12] D.W. Brenner. Empirical potential for hydrocarbons for use in simulating the chemical vapor deposition of diamond films. *Phys. Rev. B* **42** (1990) 9458–9471.

[13] E. Hairer and Chr. Lubich. The lifespan of backward error analysis for numerical integrators. *Numer. Math.* **76** (1997) 441–462.

[14] J.M. Sanz Serna. Symplectic integrators for Hamiltonian problems: an overview. *Acta Numerica* **1** (1992) 243–286.

[15] J. Tersoff. New empirical approach approach for the structure and energy of covalent systems. *Phys. Rev. B* **37** (1988) 6991–7000.

[16] J. Tersoff. Empirical interatomic potential for silicon with improved elastic constants. *Phys. Rev. B* **38** (1988) 9902–9905.

[17] J. Tersoff. Empirical interatomic potential for carbon with applications to amorphous carbon. *Phys. Rev. Lett.* **61** (1988) 2879–2882.

[18] K. Burrage. *Parallel & Sequential Methods for Ordinary Differential Equations.* Clarendon Press - Oxford, 1995.